

Accepted Manuscript

Synthesis and biological evaluation of new steroidal pyridines as potential anti-prostate cancer agents

Yun-Kai Shi, Bo Wang, Xiao-Li Shi, Yuan-Di Zhao, Bin Yu, Hong-Min Liu



PII: S0223-5234(17)31125-X

DOI: [10.1016/j.ejmech.2017.12.094](https://doi.org/10.1016/j.ejmech.2017.12.094)

Reference: EJMECH 10072

To appear in: *European Journal of Medicinal Chemistry*

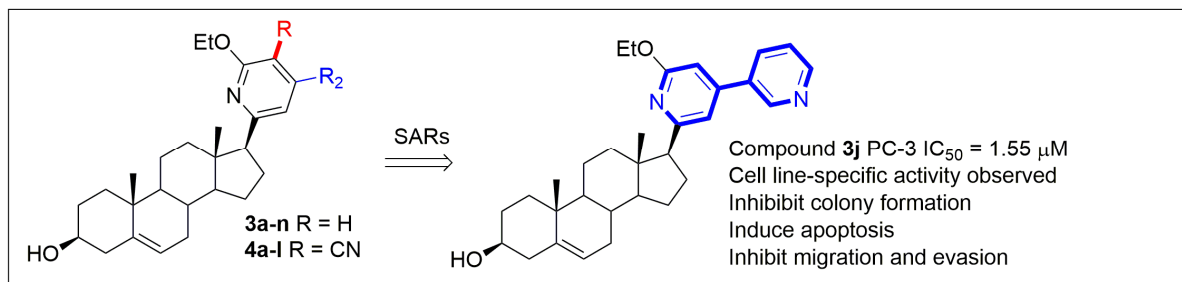
Received Date: 23 October 2017

Revised Date: 29 December 2017

Accepted Date: 30 December 2017

Please cite this article as: Y.-K. Shi, B. Wang, X.-L. Shi, Y.-D. Zhao, B. Yu, H.-M. Liu, Synthesis and biological evaluation of new steroidal pyridines as potential anti-prostate cancer agents, *European Journal of Medicinal Chemistry* (2018), doi: 10.1016/j.ejmech.2017.12.094.

This is a PDF file of an unedited manuscript that has been accepted for publication. As a service to our customers we are providing this early version of the manuscript. The manuscript will undergo copyediting, typesetting, and review of the resulting proof before it is published in its final form. Please note that during the production process errors may be discovered which could affect the content, and all legal disclaimers that apply to the journal pertain.



ACCEPTED MANUSCRIPT

Synthesis and biological evaluation of new steroidal pyridines as potential anti-prostate cancer agents

Yun-Kai Shi[#], Bo Wang[#], Xiao-Li Shi, Yuan-Di Zhao, Bin Yu*, Hong-Min Liu*

Key Laboratory of Advanced Drug Preparation Technologies (Zhengzhou University), Ministry of Education; Collaborative Innovation Center of New Drug Research and Safety Evaluation, Henan Province; School of Pharmaceutical Sciences, Zhengzhou University, Zhengzhou 450001, PR China; Key Laboratory of Henan Province for Drug Quality and Evaluation

Corresponding Authors: Dr. Bin Yu & Prof. Hong-Min Liu

E-mail: zzuyubin@hotmail.com (Bin Yu) & liuhm@zzu.edu.cn (Hong-Min Liu)

These authors contributed equally to this work.

Abstract: A series of new steroidal pyridines have been synthesized through the base-promoted three-component reaction and preliminarily evaluated for their antiproliferative activity against different types of cancer cell lines. SARs studies showed that the heterocyclic rings attached to the 4-position of the pyridine ring were preferred over the phenyl rings for the activity. Among these compounds, the most potent compound exhibited good growth inhibition against all the tested cancer cells, especially for PC-3 cells with an IC_{50} value of 1.55 μ M. Further mechanistic studies revealed that the most potent compound inhibited colony formation, migration and evasion of PC-3 cells in a concentration-dependent manner as well as induced apoptosis of PC-3 cells possibly through the mitochondria-related apoptotic pathways. Caspase-3/-9 and PARP were activated, finally leading to the apoptosis of PC-3 cells. For the AR^+ -sensitive prostate cancer cell line LNCaP, the most potent compound was less potent than abiraterone with the IC_{50} value of 8.48 and 3.29 μ M, respectively. The most potent compound could be used as a starting point for the development of new steroidal heterocycles with improved anticancer potency and selectivity. The synthesized steroidal pyridines contain the functional -OEt and CN groups, which could be used for further modifications for the construction of the steroid library.

Keywords: Steroids; Pyridines; Biaryl compounds; Antiproliferative activity; Prostate cancer

1. Introduction

Steroids, an important class of polycyclic molecules, have played key roles in regulating normal physiological processes and targeting disease-related biological sites [1, 2]. Of particular interest are steroidal heterocycles, which have drawn wide attention due to their interesting biological profiles and structural features [3-6]. Some steroidal derivatives are currently used in clinic or have advanced into clinical trials for the treatment of diseases, and two representative examples are abiraterone [7, 8] and galeterone [9, 10]. Abiraterone is presently used in clinic for the treatment of advanced prostate cancers, galeterone has advanced into phase 2 trial for the treatment of castration resistant prostate cancer (ClinicalTrials.gov Identifier: NCT01709734). Abiraterone is an androgen synthesis inhibitor by blocking the action of CYP17 enzyme, which is involved in the androgen biosynthesis [11]. Galeterone possesses a unique dual mechanism of action by selectively inhibiting the C17, 20-lyase activity of CYP17 and androgen receptor, which demonstrates good tolerance and clinically meaningful reductions in levels of prostate specific antigen (PSA).

Our group have long been devoted to the synthesis of novel steroidal derivatives and their antiproliferative evaluation [12-21], aiming to identify new steroid-based antitumor agents. Some of these compounds were found to be able to inhibit growth of human cancer cells potently and induce cell cycle arrest and apoptosis in a time-/concentration-dependent manner. One representative example is the steroidal compound **by241** bearing the spirooxindole moiety [22, 23], which exerts good *in vitro* and *in vivo* anticancer efficacy through the ROS-mediated mechanisms [24]. These findings, coupled with the anticancer profiles of abiraterone and galeterone promoted us to further explore the antitumor potential of steroidal pyridines, which were efficiently accessed from pregnenolone (PREG), aldehyde, malononitrile and sodium ethoxide (Fig. 1).

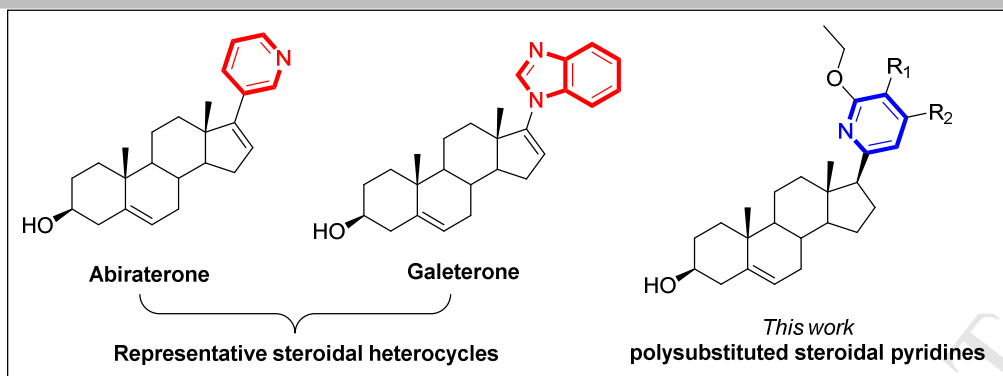
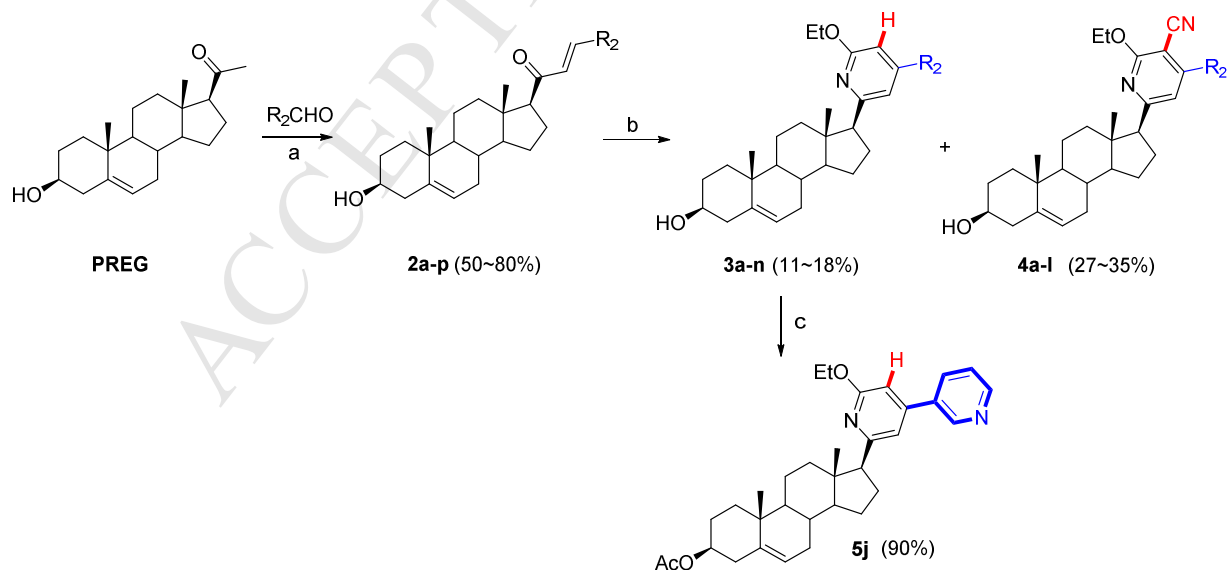


Fig. 1. Abiraterone, galeterone and the target molecules synthesized in this work.

2. Results and discussion

2.1 Chemistry

The intermediates **2a-p** were prepared in high yields *via* the $\text{Al}_2\text{O}_3/\text{KF}$ -catalyzed aldol condensation of pregnenolone (PREG) with aromatic aldehydes in ethanol following our previously reported procedures [20, 25]. Steroidal pyridines **3a-n** and **4a-l** were synthesized from steroidal α , β -unsaturated ketones **2a-p**, malononitrile and sodium ethoxide in a single operation as shown in Scheme 1. Interestingly, sodium ethoxide acted as a bifunctional species, namely the ethoxy source and the promoter of reactions between α , β -unsaturated ketones and malononitrile. The compound **5j** was also synthesized from compound **3j** through acetylation reaction, and the route is shown in Scheme 1 (See Tables 1-2 for R_2 substituents in compounds **3a-n** and **4a-l**).



Scheme 1. Synthesis of steroidal pyridines. Reagents and conditions: (a) $\text{Al}_2\text{O}_3/\text{KF}$, EtOH, reflux; (b) Malononitrile, NaOEt, EtOH, reflux; (c) Acetyl chloride, Et_3N , DMAP, DCM, r.t.

All the new compounds were characterized by ^1H , ^{13}C NMR and high-resolution mass spectra (HRMS) as described for compound **3a** (Fig. 2). In the ^1H NMR spectrum of compound **3a**, the signals of protons attached to C-18' and C-19' appeared at 0.49 and 0.93 ppm, respectively as sharp singlets. The signal of H-6' appeared at 5.29 ppm as a doublet ($J = 4.5$ Hz). Two doublets at 7.77 and 7.54 ppm, respectively had the same coupling constant ($J = 8.6$ Hz), indicating that these four protons existed in the 4-chloro phenyl group. The singlet at 4.60 ppm was assigned to the 3' α -H of steroid nucleus. The triplet and the quartet at 1.33 and 4.34 ppm, respectively were assigned to the protons attached to the ethoxy group. The proton signals attached to C-5/C-3 appeared at 7.02 and 6.86 ppm. Please refer to the 2D NMR spectra of compound **3a** included in the *Supporting Information* for details. The presence of a molecular ion peak at $m/z = 506.2817$ ($\text{M}+\text{H}$) $^+$ in the mass spectrum (calcd. 506.2826) further confirmed the structure of **3a**. It should be noted that most of the synthesized compounds were obtained as mixture of rotamers because of the twisting of biaryl compounds, which was previously observed by us [26] and other groups [27-29].

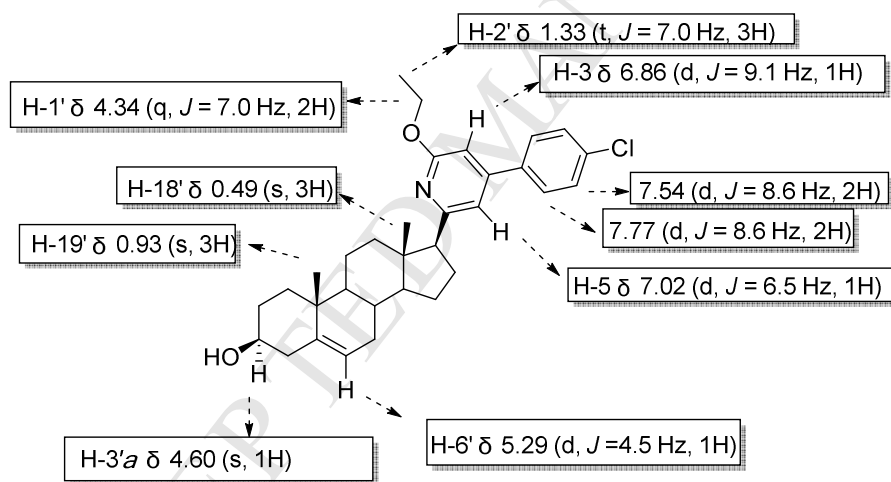
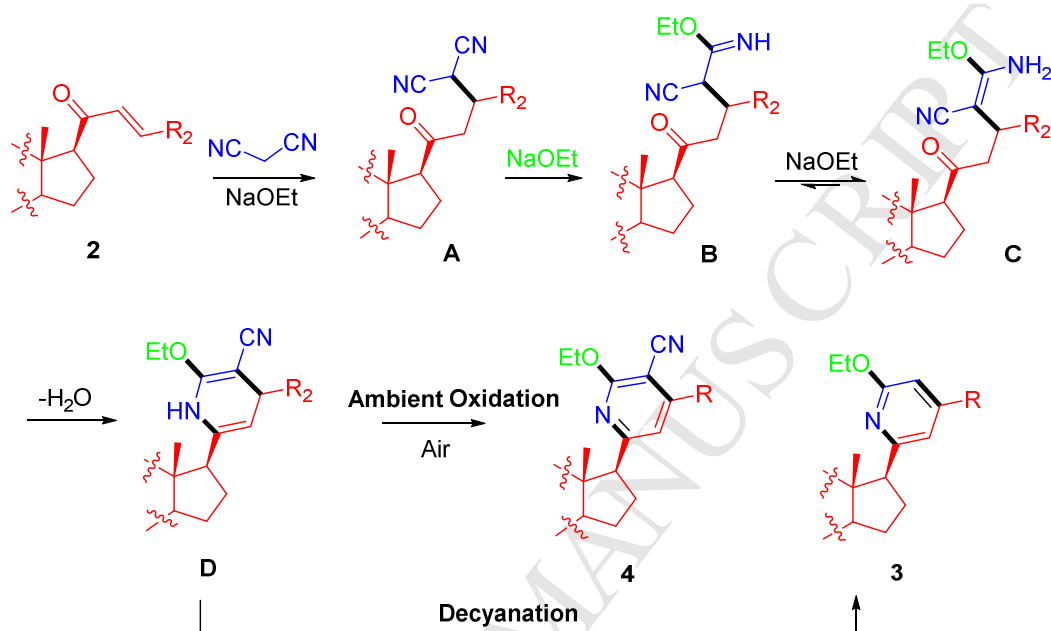


Fig. 2. Characteristic chemical shifts of compound **3a**.

Based on the interesting transformations, we also tentatively proposed the possible reaction mechanism as shown in **Scheme 2** [30, 31]. In the presence of NaOEt, the 1,4-Michael addition of malononitrile to compound **2** produced intermediate **A**, in which the CN group was attacked by NaOEt, forming the unstable intermediate **B**. Isomerization of intermediate **B** in the presence of NaOEt afforded enamine **C**, which was then subjected to the intramolecular dehydration, generating intermediate **D**. Intermediate **D** can also be oxidized under air atmosphere, forming compound **4**. Compound **3** was also generated in the reaction *via* the competitive decyanation reaction. The multisubstituted pyridine ring was formed in the reaction (The newly formed bonds were

highlighted in bold), and the -OEt and -CN group in compound **3** or **4** could be allowed for further derivatizations for the construction of the steroidal pyridine library. It was anticipated that application of different alkoxy species would provide access to new steroidal pyridines bearing various alkoxy groups. Malononitrile may also be replaced with other α -substituted acetonitriles in the reaction for the synthesis of analogs of compound **4**.



Scheme 2. Possible reaction mechanisms for the formation of steroidal pyridines.

2.2. Biological evaluation

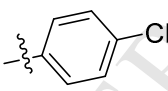
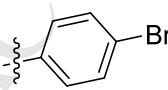
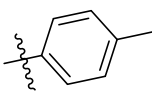
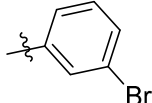
2.2.1. Antiproliferative activity

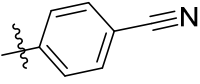
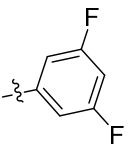
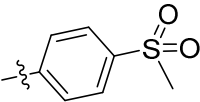
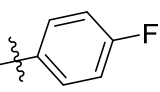
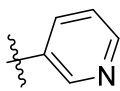
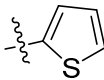
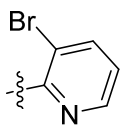
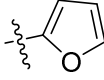
The IC₅₀ values for the synthesized compounds against three human cancer cell lines including human gastric cancer cell line (MGC-803), human prostate cancer cell line (PC-3) and human esophageal cancer cell line (EC-109) and a normal human gastric epithelial cell (GES-1) were determined using the MTT assay. The results were listed in Table 1 and the well-known anticancer drug abiraterone was used as a positive control.

As shown in Table 1, compounds **3a-i** possessing different substituted phenyl ring showed weak to moderate antiproliferative activity against the tested cancer cells. Among these compounds, compound **3g** with the 3,5-difluoro group inhibited growth of PC-3 cells with an IC₅₀ value of 16.50 μ M, around 2.8-fold less potent than abiraterone (IC₅₀ = 5.94 μ M). Interestingly, replacement of the phenyl ring with heterocyclic rings (compounds **3j-n**) significantly enhanced the antiproliferative

activity against the tested cancer cells, highlighting the importance of the heterocyclic ring for the activity. Compound **3j** bearing the pyridine ring ($IC_{50} = 1.55 \mu\text{M}$) was about 20-fold more potent than compound **3b** against PC-3 cells and also showed acceptable inhibition toward EC-109, MGC-803 cells. It is worth noting that for all the tested cancer cells, compound **3j** (also named as **SYK-001**) was even much more potent than abiraterone, a CYP17A1 inhibitor used in clinic for the treatment of advanced prostate cancers [11]. The preliminary data may warrant further development of SYK-001 as a potential anticancer lead. In contrast, compounds **3m** and **3o** had decreased activity toward the tested cancer cells, underscoring the importance of the position of the nitrogen atom for the activity. Compounds **3k** and **3n** with the thiophenyl and furanyl group, respectively were found to be less potent than compounds **3j**, **3l** and **3n**. Considering that abiraterone acetate is used in clinic as the prodrug of abiraterone, herein we also evaluated the antiproliferative activity of the acetate of compound **3j** (compound **5j**) toward the above mentioned cell lines. Compound **5j** exhibited slightly decreased antiproliferative activity against PC-3 cells compared to **3j**, but showed good selectivity to PC-3 cells over EC-109, MGC-803 cell lines and normal cell line GES-1 ($IC_{50} > 32 \mu\text{M}$).

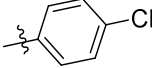
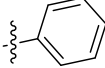
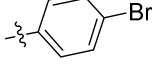
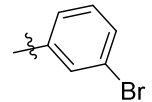
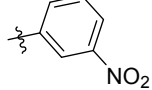
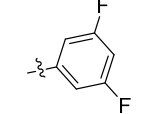
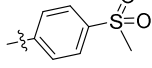
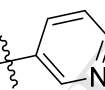
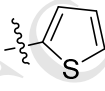
Table 1. Preliminary *in vitro* antiproliferative activities of the steroidal pyridines **3a-n** and **5j**

Compound	R ₂	IC ₅₀ (μM)			
		PC-3	EC-109	MGC-803	GES-1
3a		>32	>32	19.21±1.28	>32
3b		31.14±1.49	>32	>32	>32
3c		>32	>32	>32	>32
3d		>32	>32	>32	>32
3e		21.73±1.33	>32	>32	>32

3f		24.59±1.39	>32	23.66±1.37	>32
3g		16.50±1.21	>32	>32	>32
3h		>32	31.29±1.49	>32	>32
3i		>32	>32	>32	>32
3j		1.55±0.19	5.32±0.72	2.75±0.44	7.76±0.89
3k		15.26±1.18	17.55±1.24	>32	>32
3l		13.41±1.12	>32	25.76±1.41	>32
3m		10.78±1.03	26.24±1.41	26.08±1.41	>32
3n		6.37±0.80	16.61±1.22	4.48±0.65	15.74±1.19
5j		6.97±0.84	>32	>32	>32
Abiraterone		5.94±0.77	>32	7.72±0.88	13.12±1.11

Next, we also examined the effect of compounds **4a-1** on the antiproliferative activity against the tested cancer cell lines. As shown in Table 2, for PC-3 cells, compounds **4a-c** and **4e-g** exhibited acceptable antiproliferative activity with the IC_{50} values less than 14 μ M and were much more potent than the corresponding analogs **3a-c** and **3e, 3g**. Similarly, compounds **4j-1** bearing the heterocyclic motifs also displayed moderate antiproliferative activity. Of these compounds, compound **4b** had slightly enhanced antiproliferative activity against PC-3 cells compared to abiraterone ($IC_{50} = 4.39 \mu$ M vs. 5.94μ M). Compared to compound **3j**, compound **4j** possessing an additional -CN group attached to the 3-position of the pyridine ring was found to have decreased antiproliferative activity against the tested cancer cells.

Table 2. Preliminary *in vitro* antiproliferative activities of steroidal pyridines **4a-l**

Compound	R ₂	IC ₅₀ (μM)			
		PC-3	EC-109	MGC-803	GES-1
4a		10.43±1.02	>32	>32	>32
4b		4.39±0.64	13.31±1.12	15.76±1.19	7.80±0.89
4c		13.66±1.13	>32	>32	>32
4d		>32	>32	>32	>32
4e		9.42±0.97	>32	28.47±1.45	21.94±1.34
4f		7.77±0.89	27.56±1.44	13.05±1.11	>32
4g		6.99±0.85	19.96±1.30	12.35±1.09	>32
4h		>32	>32	>32	>32
4i		>32	>32	>32	>32
4j		5.84±0.76	2.84±0.45	14.70±1.16	>32
4k		6.98±0.84	9.84±0.99	23.61±1.37	>32
4l		12.19±1.08	10.57±1.02	22.30±1.34	30.09±1.47
Abiraterone		5.94±0.77	>32	7.72±0.88	13.12±1.11

Abiraterone acts as a partial antagonist of the androgen receptor (AR) [11], while the title compounds also possess similar structural features. Therefore, we chose prostate cancer cell line LNCaP to further evaluate the anticancer potential of compounds **3j**, **4j**, and **5j** using abiraterone as the control drug. LNCaP cells are androgen-sensitive (AR⁺) human prostate adenocarcinoma cells and have always been used as the most clinically relevant prostate cancer models that more closely mimic clinical disease [32]. As depicted in Fig. 3, compounds **3j**, **4j** and **5j** inhibited growth of LNCaP cells with the IC₅₀ value of 8.48, 5.18, 27.88 μ M, respectively, but were less potent than abiraterone, which suppressed growth of LNCaP cells with an IC₅₀ value of 3.29 μ M.

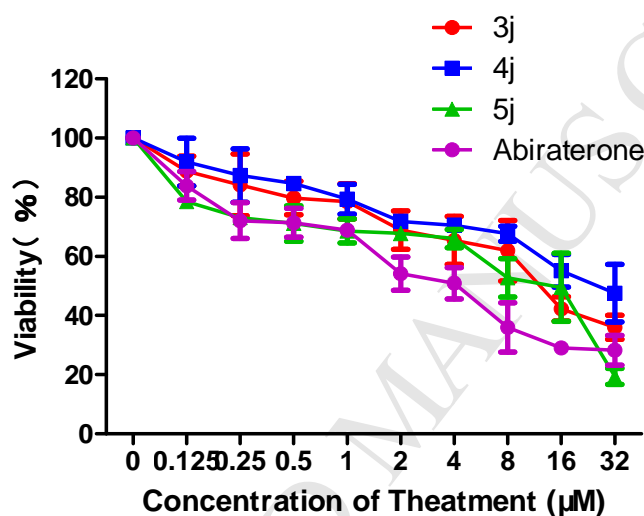


Fig. 3. Cell viability of compounds **3j**, **4j**, **5j** and abiraterone against LNCaP cells. Cells were treated with the compounds at the indicated concentrations for 72h.

2.2.2. Cell viability test and cell cycle analysis

Inspired by the favorable potency of compound **3j** toward PC-3 cells, **3j** was prioritized to perform further experiment for evaluating its antitumor potential in PC-3 cells (Fig. 4). As shown in Fig. 4A, after the treatment with **3j**, the proliferation of the PC-3 cells was significantly inhibited in a concentration and time-dependent manner. Fig. 4B showed that compound **3j** obviously inhibited colony formation of PC-3 cells. To examine the effect of different concentrations of compound **3j** on cell cycle progression against PC-3. A flow cytometric of cell-cycle assay was performed by treating PC-3 cells with various concentrations of compound **3j** (0, 0.5, 1.0, 2 μ M) for 48 h. As in shown in Fig. 4C, compound **3j** had little effect on the cell cycle arrest, indicating that the antiproliferative activity of compound **3j** was not mainly achieved by the cell cycle arrest.

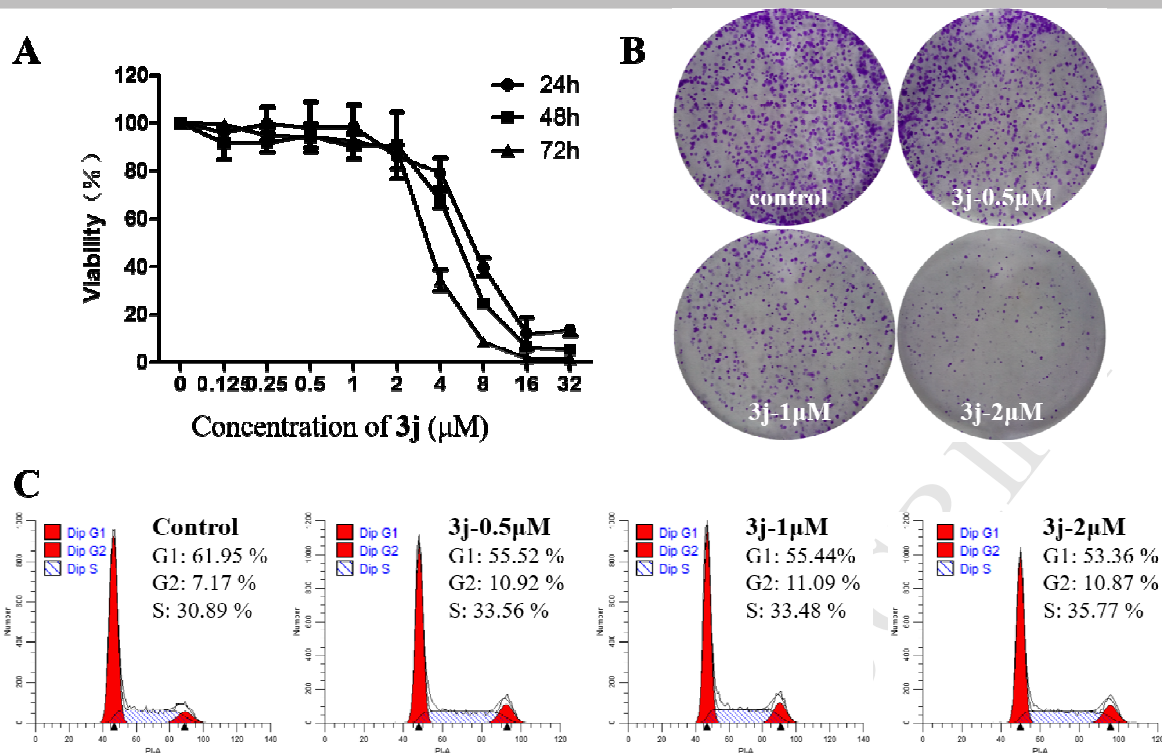
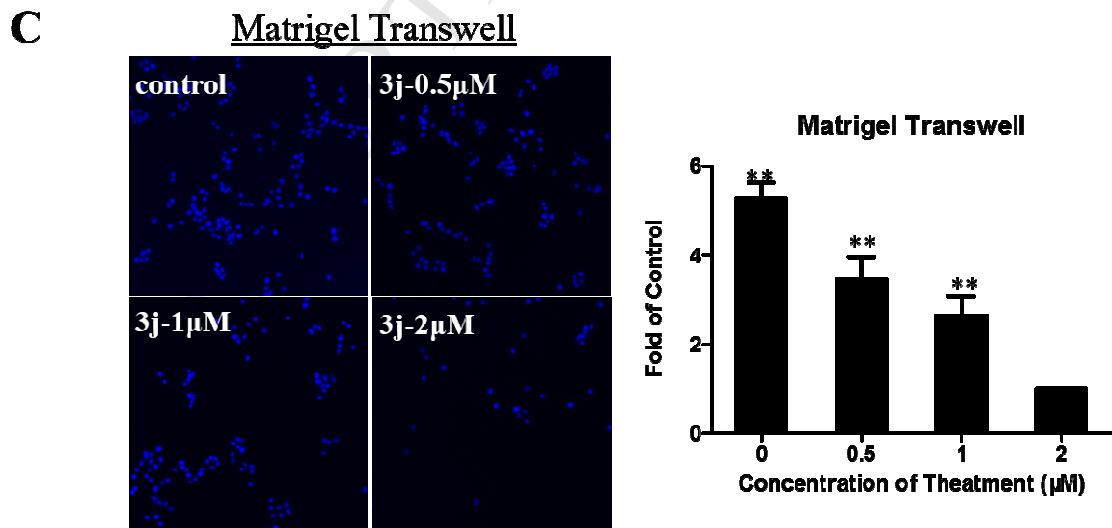
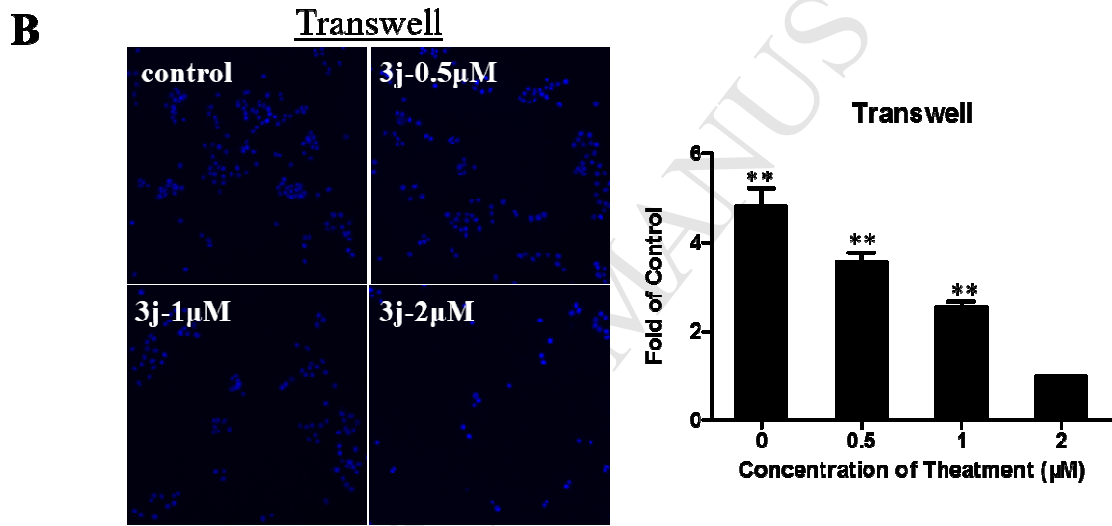
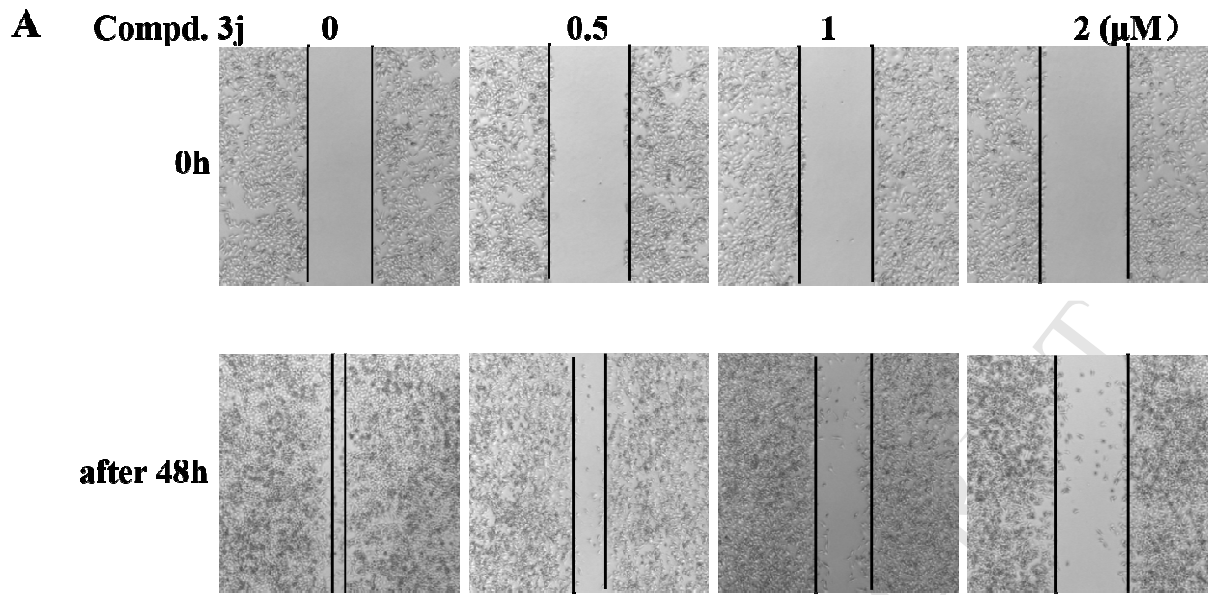


Fig. 4. Effect of compound **3j** on the proliferation of PC-3. (A) The effect of **3j** in inhibiting cell survival of PC-3 cells measured by the MTT assay. (B) The colony formation of PC-3 cells after treatment of compound **3j**. (C) Effect of compound **3j** on the cell cycle distribution of PC-3 cells. The experiments were performed three times, and a representative result is shown above.

2.2.3. Compound **3j** inhibits migration and invasion of PC-3 cells

We next investigated whether compound **3j** could inhibit the migration and invasion against PC-3 cells. Firstly, we performed the wound healing assay. As shown in Fig. 5A, after treatment of PC-3 cells with compound **3j** at different concentration (0, 0.5, 1.0, 2.0 μM) for 48 hours, the wound healings were markedly suppressed in a concentration-dependent manner. Additionally, the further transwell assay and matrigel-coated transwell assay (Fig. 5B & 5C) showed compound **3j** significantly inhibited the ability of migration and invasion of PC-3 cells concentration-dependently. Western blotting analysis (Fig. 5D) showed that compound **3j** up-regulated the expression of epithelial cells' biomarkers, E-Cadherin and Occludin, while the mesenchymal cells' biomarkers, N-Cadherin and Vimentin, were down-regulated. These results indicated that compound **3j** may block migration and invasion of PC-3 cells through inhibiting EMT process.



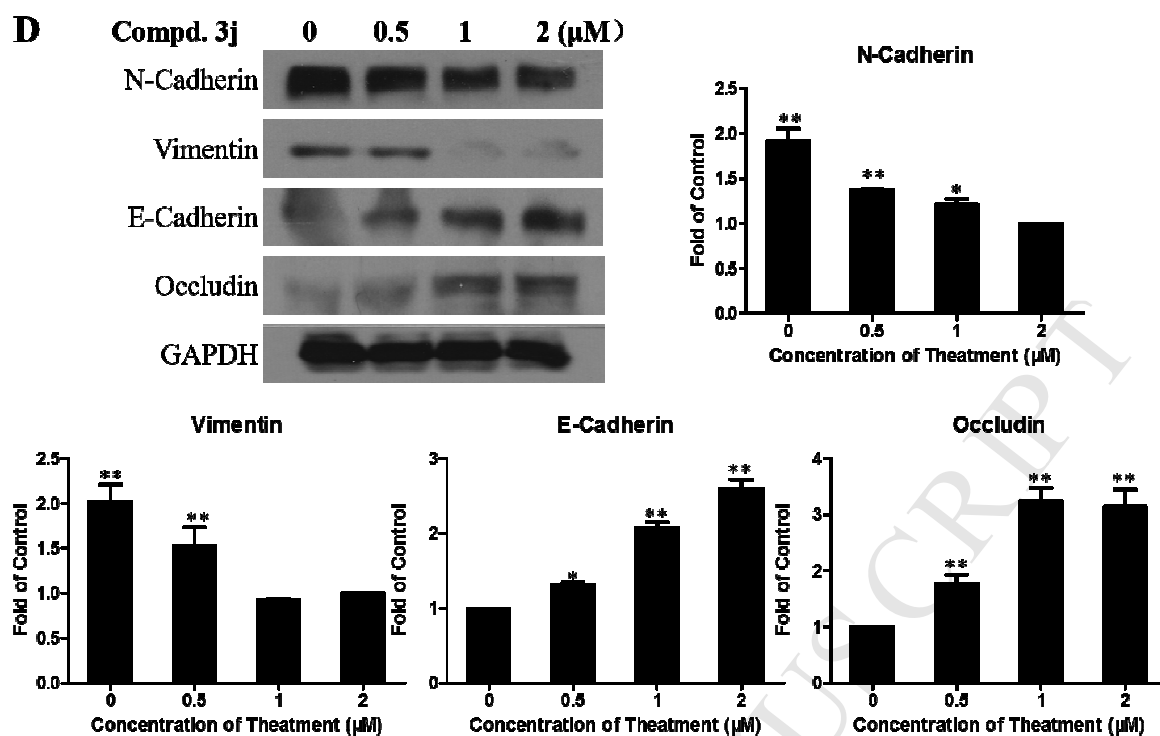


Fig. 5. Effect of compound **3j** on migration and invasion of PC-3 cells. (A) The Wound healing assay. (B and C) Migration and invasion inhibition induced by compound **3j** were reflected by the transwell and matrigel-coated transwell assays. (D) Expression of N-Cadherin, Vimentin, E-Cadherin and Occludin after treatment of compound **3j** and GAPDH was used as control. * $P < 0.05$ and ** $P < 0.01$ were considered statistically significant compared with the control. Data are mean \pm SD. All experiments were carried out at least three times.

2.2.4. Effect of compound **3j** on apoptosis and related mechanisms

Apoptosis is known as programmed cell death and typically characterized by distinctive cell morphological changes. Compound **3j** was chosen for evaluating its ability of inducing apoptosis. The Hoechst 33258 staining was performed to investigate morphological changes of PC-3 cells. After 48h incubation with compound **3j** at indicated concentrations, characteristic apoptotic morphological changes were observed, including cell rounding, chromatin shrinkage and formation of apoptotic bodies (Fig. 6A), particularly at high concentrations. To further explore the effect of compound **3j** on cell apoptosis, we performed the flow cytometry analysis by AnnexinV-FITC/PI double staining. As shown in Fig. 6B, after treatment with compound **3j** for 48h at different concentrations (0, 0.5, 1.0, 2.0 μM), the percentage of apoptotic PC-3 cells (including early phase and late phase apoptosis) were increased up to 13.3%, 20.8%, and 22.2%, respectively. The results showed that compound **3j** could increase the cellular apoptosis in a concentration-independent manner. Next, the western blotting analysis was performed to examine the expression of apoptosis related proteins. As shown in Fig. 6C, treatment of PC-3 cells with compound **3j** activated caspase 9

and caspase 3 in a concentration-dependent manner, which then finally activate PARP. The data suggest that the apoptosis caused by compound **3j** may be involved in mitochondria-related apoptosis pathway. While the expression of p53 was almost unchanged.

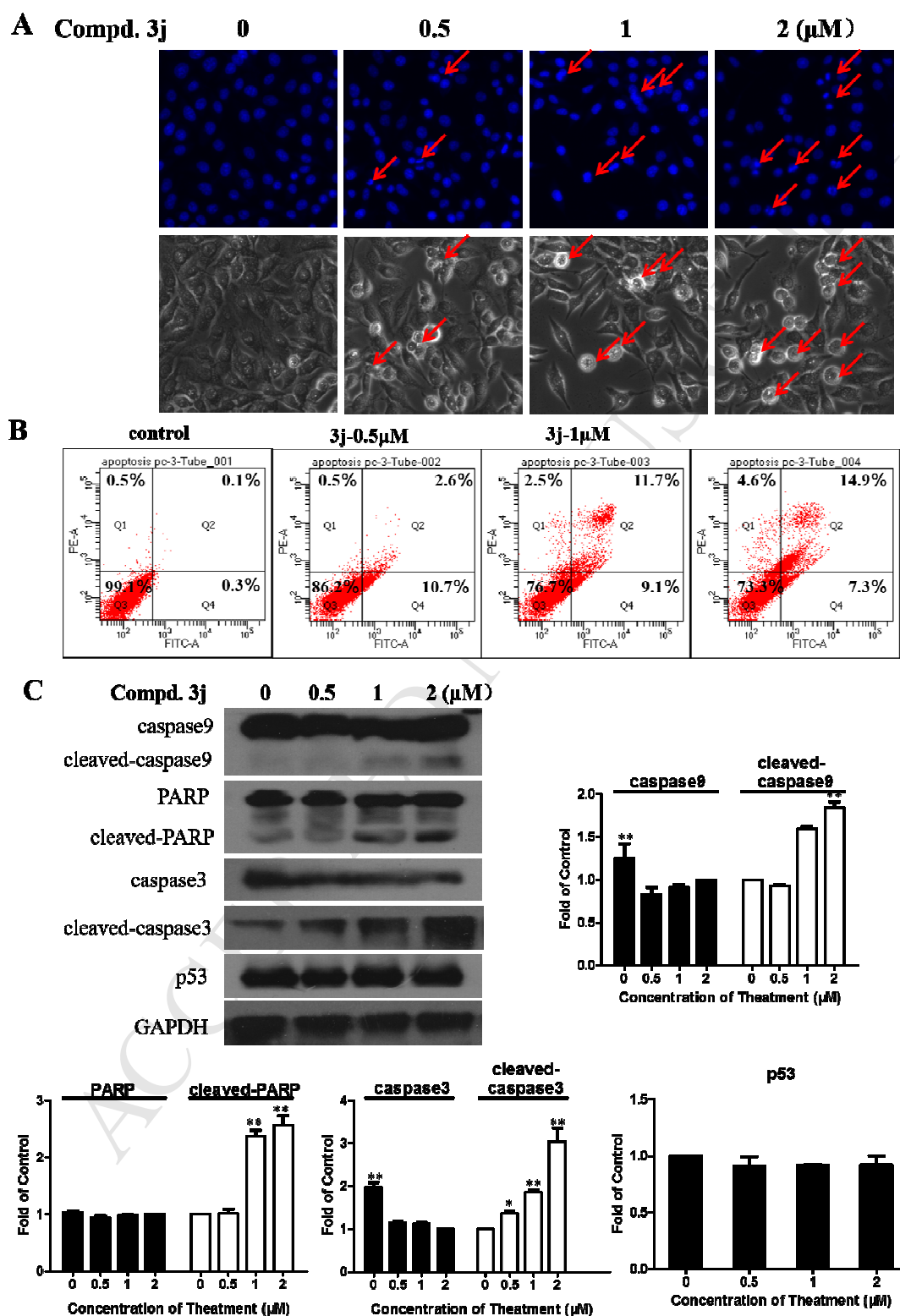


Fig. 6. Compound **3j** induced apoptosis of PC-3 cells. (A) Apoptosis analysis with Hoechst-33258 staining. (B) Apoptosis effect on human PC-3 cell line induced by compound **3j**. Apoptotic cells were detected with Annexin V-FITC/PI double staining after incubation with compound **3j**. The lower left quadrants represent live cells, the

lower right quadrants are for early/primary apoptotic cells, upper right quadrants are for late/secondary apoptotic cells, while the upper left quadrants represent cells damaged during the procedure. (C) Expression of apoptosis involved protein, caspase 9, cleaved-caspase 9, PARP, cleaved-PARP, caspase 3, cleaved-caspase 3 and p53 were determined after treatment with compound **3j**. The GAPDH was used as control. * $P < 0.05$ and ** $P < 0.01$ were considered statistically significant compared with the control. Dates are mean \pm SD. All experiments were carried out at least three times.

3. Conclusions

Following our previous work in the identification of new steroidal heterocycles for cancer therapy and inspired by the anticancer efficacy of abiraterone and galeterone, we herein reported the synthesis of new steroidal pyridines through the base-promoted three-component one-pot reaction, in which a new multisubstituted pyridine ring was formed. Biological evaluation indicated that the synthesized steroidal pyridines showed varied antiproliferative activity against the tested cancer cells dependent on the substituents attached. SARs studies showed that the heterocyclic rings attached to the 4-position of the pyridine ring were preferred over the phenyl rings for the activity. Among these compounds, compound **3j** possessing an additional pyridine ring at the *p*-position exhibited good growth inhibition against all the tested cancer cells, especially for PC-3 cells with an IC_{50} value of 1.55 μ M. Further mechanistic studies revealed that compound **3j** inhibited colony formation, migration and evasion of PC-3 cells in a concentration-dependent manner. E-Cadherin and Occludin were found to be up-regulated in PC-3 cells when treated with **3j**, while the expression of N-Cadherin and Vimentin was down-regulated accordingly. Compound **3j** induced apoptosis of PC-3 cells possibly through the mitochondria-related apoptotic pathways. Caspase-3/-9 and PARP were activated, which then finally led to apoptosis of PC-3 cells, while the expression of p53 was almost unchanged. However, compound **3j** had little effect on the cell cycle arrest of PC-3 cells. For the AR⁺-sensitive prostate cancer cell line LNCaP, compound **3j** inhibited growth with an IC_{50} value of 8.48 μ M, slightly less potent than the anti-prostate cancer drug abiraterone (IC_{50} = 3.29 μ M). The synthesized steroidal pyridines contain the -OEt and CN groups, which could be allowed for further modifications for the construction of the steroid library. Compound **3j** could be used as a starting point for the development of new steroidal heterocycles with improved anticancer potency and selectivity.

4. Experimental section

4.1. General

Reagents and solvents were purchased from commercial sources and were used without further purification. Thin-layer chromatography (TLC) was carried out on glass plates coated with silica gel and visualized by UV light (254 nm). The products were purified by column chromatography over silica gel. Melting points were determined on a Beijing Keyi XT4A apparatus and are uncorrected. All the NMR spectra were recorded with a Bruker DPX 400 MHz spectrometer with TMS as internal standard in CDCl₃ or DMSO-*d*₆. Chemical shifts are given as δ ppm values relative to TMS (Most of the peaks due to the complexity of the steroidal skeleton are merged and therefore could not be differentiated. Thus δ values of only those peaks that could distinguish the product are reported). *The ¹H-NMR data of the major rotamer were given.* High-resolution mass spectra (HRMS) were recorded on a Waters Micromass Q-T of Micromass spectrometer by electrospray ionization (ESI).

4.2. General procedure for the synthesis of compounds **3a-n** and **4a-l**

The mixture of malononitrile (1.1 mmol, 1.1 eq), appropriate steroidal α,β -unsaturated ketone (1.0mmol, 1.0 eq) and sodium ethoxide (4.0 mmol, 4.0 eq) was refluxed for 8 h in ethanol and monitored by TLC. After the completion of the reaction, the reaction mixture was cooled to room temperature and filtrated with ethanol, then washed with ethanol. The filtrate was concentrated under reduced vacuum. The residue was purified by column chromatography (PE: Acetone = 4:1) to give the target products.

4.2.1. 2-Ethoxyl-4-(4-chlorophenyl)-6-[(3' β , 17' β)-3'-(hydroxyl) androst-5'-en-17'-yl] pyridine (**3a**)

White solid, yield 17%, m.p.89.1-90.8 $^{\circ}$. ¹H NMR (400 MHz, DMSO-*d*₆) δ 7.77 (d, J = 8.6 Hz, 2H), 7.54 (d, J = 8.6 Hz, 2H), 7.02 (s, 1H), 6.86 (s, 1H), 5.31 (d, J = 4.6 Hz, 1H), 4.60 (s, 1H), 4.34 (q, J = 7.0 Hz, 2H), 1.33 (t, J = 7.0 Hz, 3H), 0.93 (s, 3H), 0.49 (s, 3H). ¹³C NMR (100 MHz, DMSO-*d*₆) δ 162.92, 159.55, 148.65, 141.32, 136.54, 133.81, 128.98, 128.66, 120.32, 113.77, 104.77, 69.97, 60.91, 57.15, 56.09, 49.88, 44.26, 42.21, 37.62, 36.94, 36.15, 31.72, 31.40, 29.01, 24.50, 24.29, 20.38, 19.16, 14.57, 12.86. HRMS (ESI):m/z calcd for C₃₂H₄₁ClNO₂ (M+H)⁺, 506.2826 ; found, .506.2817.

4.2.2. 2-Ethoxyl-4-phenyl-6-[(3' β , 17' β)-3'-(hydroxyl) androst-5'-en-17'-yl] pyridine (**3b**)

White solid, yield 15%, m.p.100.9-102.7 $^{\circ}$ C. ^1H NMR (400 MHz, CDCl_3) δ 7.58 – 7.49 (m, 2H), 7.41 – 7.29 (m, 3H), 6.90 (s, 1H), 6.74 (s, 1H), 5.30 (d, $J = 5.9$ Hz, 1H), 4.34 (q, $J = 7.0$ Hz, 2H), 3.54 – 3.38 (m, 1H), 1.40 (t, $J = 7.0$ Hz, 3H), 0.93 (s, 3H), 0.49 (s, 3H). ^{13}C NMR (100 MHz, CDCl_3) δ 163.38, 159.75, 150.73, 140.91, 139.18, 128.87, 128.57, 127.05, 121.63, 114.56, 105.40, 71.77, 61.46, 58.07, 56.80, 50.42, 44.84, 42.32, 38.26, 37.33, 36.65, 32.24, 32.00, 31.67, 29.72, 26.94, 25.08, 24.76, 20.97, 20.91, 19.45, 19.42, 14.83, 13.03. HRMS (ESI):m/z calcd for $\text{C}_{32}\text{H}_{42}\text{NO}_2$ ($\text{M}+\text{H}$) $^+$, 472.3216 ; found, 472.3213.

4.2.3. 2-Ethoxyl-4-(4-bromophenyl)-6-[(3' β , 17' β)-3'-(hydroxyl) androst-5'-en-17'-yl] pyridine (**3c**)

White solid, yield 18%, m.p.80.3-82.0 $^{\circ}$ C. ^1H NMR (400 MHz, CDCl_3) δ 7.50 (d, $J = 8.5$ Hz, 2H), 7.41 – 7.36 (m, 2H), 6.77 (s, 1H), 6.71 (s, 1H), 6.60 (d, $J = 9.6$ Hz, 1H), 5.31 (d, $J = 5.2$ Hz, 1H), 4.34 (q, $J = 7.0$ Hz, 2H), 3.53 – 3.41 (m, 1H), 1.33 (t, $J = 7.0$ Hz, 3H), 0.93 (s, 3H), 0.48 (s, 3H). ^{13}C NMR (100 MHz, CDCl_3) δ 162.39, 159.04, 148.46, 139.85, 137.06, 131.00, 127.60, 121.88, 120.60, 113.15, 104.21, 70.77, 60.51, 57.02, 55.76, 49.36, 43.84, 41.28, 37.20, 36.28, 35.61, 31.19, 30.95, 30.64, 28.68, 24.05, 23.71, 21.67, 19.86, 18.42, 13.76, 13.10, 12.00. HRMS (ESI):m/z calcd for $\text{C}_{32}\text{H}_{41}\text{BrNO}_2$ ($\text{M}+\text{H}$) $^+$ 550.2321 ; found, 550.2321.

4.2.4. 2-Ethoxyl-4-(4-methylphenyl)-6-[(3' β , 17' β)-3'-(hydroxyl) androst-5'-en-17'-yl]pyridine (**3d**)

White solid, yield 13%, m.p.85.3-87.2 $^{\circ}$ C. ^1H NMR (400 MHz, CDCl_3) δ 7.50 (d, $J = 7.8$ Hz, 2H), 7.25 (d, $J = 5.2$ Hz, 2H), 6.90 (s, 1H), 6.73 (s, 1H), 5.38 (s, 1H), 4.40 (q, $J = 7.0$ Hz, 1H), 3.42-3.60 (m, 1H), 2.40 (s, 3H), 1.41 (t, $J = 7.0$ Hz, 3H), 1.01 (s, 3H), 0.56 (s, 3H). ^{13}C NMR (100 MHz, CDCl_3) δ 163.35, 140.88, 140.81, 129.60, 126.89, 121.65, 114.44, 71.82, 56.78, 50.40, 49.96, 44.85, 42.31, 37.31, 36.64, 36.58, 34.84, 32.62, 32.32, 32.23, 31.99, 31.93, 31.67, 29.71, 29.37, 24.75, 22.70, 21.21, 20.89, 19.44, 14.81, 14.12, 13.02. HRMS (ESI):m/z calcd for $\text{C}_{33}\text{H}_{44}\text{NO}_2$ ($\text{M}+\text{H}$) $^+$ 486.3372 ; found, 486.3373.

4.2.5. 2-Ethoxyl-4-(3-bromophenyl)-6-[(3' β , 17' β)-3'-(hydroxyl) androst-5'-en-17'-yl]pyridine (**3e**)

White solid, yield 15%, m.p.89.2-91.3 $^{\circ}$ C. ^1H NMR (400 MHz, CDCl_3) δ 7.72 (t, $J = 1.7$ Hz, 1H), 7.54 – 7.49 (m, 2H), 7.30 (t, $J = 7.9$ Hz, 1H), 6.84 (s, 1H), 6.69 (s, 1H), 5.37 (d, $J = 5.2$ Hz, 1H), 4.40 (q, $J = 7.0$ Hz, 2H), 3.60 – 3.46 (m, 1H), 1.40 (t, $J = 7.0$ Hz, 3H), 1.00 (s, 3H), 0.55 (s, 3H). ^{13}C

NMR (100 MHz, CDCl₃) δ 163.38, 160.10, 149.23, 141.28, 140.84, 131.51, 130.40, 130.11, 125.69, 123.01, 121.72, 121.64, 114.28, 105.48, 71.90, 61.60, 58.03, 56.77, 50.37, 44.89, 42.21, 38.23, 37.31, 36.63, 32.21, 31.98, 31.57, 29.72, 25.13, 24.75, 20.89, 19.45, 14.80, 13.05. HRMS (ESI):m/z calcd for C₃₂H₄₁BrNO₂ (M+H)⁺ 550.2321 ; found, 550.2321.

4.2.6. 2-Ethoxyl-4-(4-cyanophenyl)-6-[(3' β , 17' β)-3'-(hydroxyl) androst-5'-en-17'-yl]pyridine (**3f**)

White solid, yield 17%, m.p.92.2-94.4 \square . ¹H NMR (400 MHz, CDCl₃) δ 7.74 (d, *J* = 8.4 Hz, 2H), 7.68 (d, *J* = 8.4 Hz, 2H), 6.86 (s, 1H), 6.71 (s, 1H), 5.38 (d, *J* = 5.0 Hz, 1H), 4.42 (q, *J* = 7.0 Hz, 2H), 3.60 – 3.48 (m, 1H), 1.41 (t, *J* = 7.0 Hz, 3H), 1.01 (s, 3H), 0.55 (s, 3H). ¹³C NMR (100 MHz, CDCl₃) δ 163.46, 160.51, 148.65, 143.71, 140.89, 132.69, 127.78, 121.57, 118.63, 114.18, 112.22, 105.71, 71.74, 61.68, 58.07, 56.78, 50.35, 44.92, 42.28, 38.24, 37.30, 36.62, 32.20, 31.96, 31.64, 25.08, 24.73, 20.87, 19.44, 14.76, 13.05. HRMS (ESI):m/z calcd for C₃₃H₄₁N₂O₂ (M+H)⁺ 497.3168 ; found, 497.3169.

4.2.7. 2-Ethoxyl-4-(3,5-difluorophenyl)-6-[(3' β ,17' β)-3'-(hydroxyl) androst-5'-en-17'-yl] pyridine (**3g**)

White solid, yield 16%, m.p.88.7-90.6 \square . ¹H NMR (400 MHz, CDCl₃) δ 7.10 (d, *J* = 6.3 Hz, 2H), 6.81 (m, 2H), 6.67 (s, 1H), 5.38 (d, *J* = 2.9 Hz, 1H), 4.40 (q, *J* = 7.0 Hz, 2H), 3.63 – 3.52 (m, 1H), 1.39 (t, *J* = 7.0 Hz, 3H), 1.00 (s, 3H), 0.55 (s,3H). ¹³C NMR (100 MHz, CDCl₃) δ 164.60, 164.47, 163.46, 162.13, 162.00, 160.36, 148.31, 142.50, 140.78, 121.68, 113.99, 110.12, 110.05, 109.93, 109.86, 105.48, 103.78, 72.06, 61.65, 58.04, 56.78, 50.37, 44.90, 42.10, 38.23, 37.30, 36.62, 32.21, 31.97, 31.47, 29.73, 25.09, 24.74, 20.90, 19.43, 14.75, 13.03. HRMS (ESI):m/z calcd for C₃₂H₄₀F₂NO₂ (M+H)⁺ 508.3027 ; found, 508.3029.

4.2.8.2-Ethoxyl-4-(4-methylsulfonylphenyl)-6-[(3' β ,17' β)-3'-(hydroxyl)androst-5'-en-17'-yl]pyridine (**3h**)

White solid, yield 16%, m.p.113.1-114.9 \square . ¹H NMR (400 MHz, CDCl₃) δ 8.03 (d, *J* = 8.4 Hz, 2H), 7.78 (d, *J* = 8.4 Hz, 2H), 6.84 (s, 1H), 6.73 (s, 1H), 5.36 (s, 1H), 4.41 (q, *J* = 7.0 Hz, 2H), 3.64 – 3.46 (m, 1H), 3.11 (s, 3H), 1.41 (t, *J* = 7.0 Hz, 3H), 0.99 (s, 3H), 0.98 (s, 3H). ¹³C NMR (100 MHz, CDCl₃) δ 163.49, 163.44, 144.52, 140.69, 140.36, 128.08, 128.00, 121.69, 114.65, 105.56, 72.05, 61.76, 56.70, 50.62, 49.94, 45.77, 44.54, 41.98, 37.16, 36.54, 34.86, 32.61, 32.28, 31.35, 29.68,

27.58, 26.47, 20.92, 19.39, 14.89. HRMS (ESI):*m/z* calcd for C₃₃H₄₃NO₄SNa (M+Na)⁺ 572.2810; found, 572.2812.

4.2.9. 2-Ethoxyl-4-(4-fluorophenyl)-6-[(3 β , 17 β)-3'-(hydroxyl) androst-5'-en-17'-yl] pyridine (**3i**)

White solid, yield 17%, m.p.195.4-197.9 \square . ¹H NMR (400 MHz, CDCl₃) δ 7.61 – 7.51 (m, 2H), 7.13 (t, *J* = 8.5 Hz, 2H), 6.78 (s, 1H), 6.68 (s, 1H), 5.38 (d, *J* = 4.8 Hz, 1H), 4.41 (q, *J* = 7.0 Hz, 2H), 3.58 – 3.50 (m, 1H), 1.40 (t, *J* = 7.0 Hz, 3H), 1.01 (s, 3H), 0.56 (s, 3H). ¹³C NMR (100 MHz, CDCl₃) δ 163.40, 159.91, 149.66, 140.90, 135.27, 128.76, 128.68, 121.62, 115.92, 115.71, 114.34, 105.29, 71.78, 61.49, 58.06, 56.80, 50.41, 44.84, 42.32, 38.27, 37.32, 36.64, 32.23, 31.99, 31.67, 29.71, 25.08, 24.75, 20.91, 19.44, 14.81, 13.02. HRMS (ESI):*m/z* calcd for C₃₂H₄₁FNO₂ (M+H)⁺ 490.3121 ; found, 490.3122.

4.2.10. 2-Ethoxyl-4-(pyridin-3-yl)-6-[(3 β , 17 β)-3'-(hydroxyl) androst-5'-en-17'-yl]pyridine (**3j**)

White solid, yield 13%, m.p.122.5-124.2 \square . ¹H NMR (400 MHz, CDCl₃) δ 8.94 (d, *J* = 1.8 Hz, 1H), 8.74 (d, *J* = 5.0 Hz, 1H), 8.05 – 7.97 (m, 1H), 7.52 (d, *J* = 5.1 Hz, 1H), 6.86 (s, 1H), 6.72 (s, 1H), 5.37 (d, *J* = 5.0 Hz, 1H), 4.42 (q, *J* = 7.0 Hz, 2H), 3.62 – 3.47 (m, 1H), 1.40 (t, *J* = 7.0 Hz, 3H), 1.00 (s, 3H), 0.55 (s, 3H). ¹³C NMR (100 MHz, CDCl₃) δ 163.47, 160.74, 148.91, 147.62, 146.31, 140.96, 136.31, 135.95, 124.61, 121.48, 114.08, 105.66, 71.65, 61.68, 58.04, 56.77, 50.34, 44.94, 42.30, 38.20, 37.32, 36.63, 32.20, 31.95, 31.92, 31.63, 29.69, 25.09, 24.72, 20.87, 19.44, 14.73, 13.04. HRMS (ESI):*m/z* calcd for C₃₁H₄₁N₂O₂ (M+H)⁺ 473.3168 ; found, 473.3157.

4.2.11. 2-Ethoxyl-4-(thiofuran-2-yl)-6-[(3 β , 17 β)-3'-(hydroxyl) androst-5'-en-17'-yl]pyridine (**3k**)

White solid, yield 18%, m.p.90.2-92.1 \square . ¹H NMR (400 MHz, CDCl₃) δ 7.45 – 7.40 (m, 1H), 7.34 (d, *J* = 5.0 Hz, 1H), 7.11 – 7.07 (m, 1H), 6.74 (s, 1H), 6.72 (s, 1H), 5.37 (d, *J* = 5.3 Hz, 1H), 4.39 (q, *J* = 6.9 Hz, 2H), 3.58 – 3.45 (m, 1H), 1.39 (t, *J* = 7.0 Hz, 3H), 1.00 (s, 3H), 0.54 (s, 3H). ¹³C NMR (100 MHz, CDCl₃) δ 163.42, 160.03, 143.43, 142.24, 140.89, 128.08, 126.25, 124.69, 121.63, 113.05, 103.72, 71.79, 61.50, 57.92, 56.78, 56.67, 50.57, 50.39, 49.97, 45.68, 44.86, 42.31, 38.20, 37.31, 36.63, 32.21, 31.98, 31.64, 24.99, 24.74, 20.90, 19.45, 14.81, 13.01. HRMS (ESI):*m/z* calcd for C₃₀H₄₀NO₂S (M+H)⁺ 478.2780 ; found, 478.2781.

4.2.12. 2-Ethoxyl-4-(3-bromopyridin-2-yl)-6-[(3' β ,17' β)-3'-(hydroxyl) androst-5'-en-17'-yl] pyridine (**3l**)

White solid, yield 13%, m.p.90.9-92.8 $^{\circ}$. ^1H NMR (400 MHz, CDCl_3) δ 7.67 (d, $J = 7.6$ Hz, 1H), 7.61 (t, $J = 7.7$ Hz, 1H), 7.48 (d, $J = 7.7$ Hz, 1H), 7.26 (s, 1H), 7.08 (s, 1H), 5.43 – 5.33 (m, 1H), 4.41 (q, $J = 7.1$ Hz, 2H), 3.60 – 3.44 (m, 1H), 1.42 (t, $J = 7.0$ Hz, 3H), 1.00 (s, 3H), 0.55 (s, 3H). ^{13}C NMR (100 MHz, CDCl_3) δ 163.56, 160.37, 156.87, 147.18, 142.32, 140.89, 139.04, 127.74, 121.63, 119.59, 113.59, 105.37, 71.79, 61.62, 58.04, 56.79, 50.39, 44.92, 42.32, 38.23, 37.31, 36.63, 32.22, 31.98, 31.68, 25.13, 24.75, 20.91, 19.44, 14.77, 13.05. HRMS (ESI):m/z calcd for $\text{C}_{31}\text{H}_{40}\text{BrN}_2\text{O}_2$ (M+H) $^+$ 551.2273 ; found, 551.2274 .

4.2.13. 2-Ethoxyl-4-(furan-2-yl)-6-[(3' β , 17' β)-3'-(hydroxyl) androst-5'-en-17'-yl]pyridine (**3m**)

White solid, yield 15%, m.p.85.7-87.6 $^{\circ}$. ^1H NMR (400 MHz, CDCl_3) δ 7.49 (s, 1H), 6.96 – 6.87 (m, 1H), 6.78 (m, 2H), 6.49 (s, 1H), 5.38 (d, $J = 5.2$ Hz, 1H), 4.40 (q, $J = 7.1$ Hz, 2H), 3.61 – 3.46 (m, 1H), 1.39 (t, $J = 7.0$ Hz, 3H), 1.00 (s, 3H), 0.54 (s, 3H). ^{13}C NMR (100 MHz, CDCl_3) δ 163.35, 159.93, 152.26, 143.10, 140.88, 139.65, 121.63, 111.79, 110.75, 107.81, 100.56, 71.79, 61.46, 57.96, 56.76, 50.39, 44.82, 42.29, 38.23, 37.30, 36.63, 32.20, 31.97, 31.64, 24.97, 24.73, 20.93, 19.44, 14.80, 12.99. HRMS (ESI):m/z calcd for $\text{C}_{30}\text{H}_{40}\text{NO}_3$ (M+H) $^+$ 462.3008 ; found, 462.3007 .

4.2.14. 2-Ethoxyl-4-(pyridin-4-yl)-6-[(3' β , 17' β)-3'-(hydroxyl) androst-5'-en-17'-yl]pyridine (**3n**)

White solid, yield 11%, m.p.95.3-97.6 $^{\circ}$. ^1H NMR (400 MHz, CDCl_3) δ 8.86 (d, $J = 4.9$ Hz, 2H), 7.69 (d, $J = 4.9$ Hz, 2H), 6.88 (s, 1H), 6.75 (s, 1H), 5.37 (d, $J = 5.1$ Hz, 1H), 4.43 (q, $J = 7.0$ Hz, 2H), 3.60 – 3.46 (m, 1H), 1.40 (t, $J = 7.0$ Hz, 3H) 1.00 (s, 3H), 0.55 (s, 3H). ^{13}C NMR (100 MHz, CDCl_3) δ 163.57, 161.18, 149.35, 146.23, 140.93, 123.02, 121.47, 113.68, 105.77, 71.66, 61.85, 58.08, 56.76, 50.32, 44.99, 42.26, 38.20, 37.30, 36.61, 32.19, 31.92, 31.61, 29.69, 25.11, 24.71, 22.68, 20.85, 19.43, 14.69, 13.05. HRMS (ESI):m/z calcd for $\text{C}_{31}\text{H}_{41}\text{N}_2\text{O}_2$ (M+H) $^+$ 473.3168 ; found, 473.3167.

4.2.15. 2-Ethoxyl-3-cyano-4-(4-chlorophenyl)-6-[(3' β , 17' β)-3'-(hydroxyl) androst-5'-en-17'-yl]pyridine (**4a**)

White solid, yield 33%, m.p.117.8-119.6 $^{\circ}$. ^1H NMR (400 MHz, CDCl_3) δ 7.52 (d, $J = 8.5$ Hz, 2H), 7.47 (d, $J = 6.6$ Hz, 2H), 6.77 (s, 1H), 5.37 (s, 1H), 4.54 (q, $J = 7.0$ Hz, 2H), 3.56-3.52 (m, 1H),

1.45 (t, $J = 8.0$ Hz, 3H), 1.01 (s, 3H), 0.56 (s, 3H). ^{13}C NMR (100 MHz, CDCl_3) δ 164.75, 164.13, 153.88, 140.85, 136.05, 134.90, 129.75, 129.16, 121.47, 116.41, 115.60, 91.69, 71.85, 63.22, 58.46, 56.90, 50.25, 45.62, 42.17, 38.20, 37.28, 36.60, 32.19, 31.90, 31.54, 29.26, 25.01, 24.72, 20.86, 19.42, 14.53, 13.13. HRMS (ESI): m/z calcd for $\text{C}_{33}\text{H}_{39}\text{ClN}_2\text{O}_2\text{Na}$ ($\text{M}+\text{Na}$) $^+$ 553.2598 ; found, 553.2596.

4.2.16. 2-Ethoxyl-3-cyano-4-phenyl-6-[(3 β , 17' β)-3'-(hydroxyl) androst-5'-en-17'-yl]pyridine (**4b**)

White solid, yield 35%, m.p.100.9-102.4 $^{\circ}\text{C}$. ^1H NMR (400 MHz, CDCl_3) δ 7.58 (d, $J = 6.6$ Hz, 2H), 7.48 (d, $J = 5.9$ Hz, 3H), 6.81 (s, 1H), 5.36 (s, 1H), 4.53 (q, $J = 7.0$ Hz, 2H), 3.61-3.54 (m, 1H), 1.45 (t, $J = 8.0$ Hz, 3H), 1.00 (s, 3H), 0.56 (s, 3H). ^{13}C NMR (100 MHz, CDCl_3) δ 182.96, 167.30, 164.22, 155.01, 140.86, 129.70, 128.85, 128.42, 121.48, 117.06, 71.74, 63.10, 58.45, 57.20, 56.91, 50.90, 50.29, 49.96, 46.37, 45.57, 42.24, 36.59, 34.93, 32.31, 31.65, 27.42, 26.93, 26.45, 21.00, 20.88, 19.41, 14.72, 13.13. HRMS (ESI): m/z calcd for $\text{C}_{33}\text{H}_{41}\text{N}_2\text{O}_2$ ($\text{M}+\text{H}$) $^+$ 497.3168 ; found, 497.3167.

4.2.17. 2-Ethoxyl-3-cyano-4-(4-bromophenyl)-6-[(3 β , 17' β)-3'-(hydroxyl) androst-5'-en-17'-yl]pyridine (**4c**)

White solid, yield 28%, m.p.115.9-117.4 $^{\circ}\text{C}$. ^1H NMR (400 MHz, CDCl_3) δ 7.62 (d, $J = 7.1$ Hz, 2H), 7.45 (d, $J = 8.2$ Hz, 2H), 6.77 (s, 1H), 5.36 (s, 1H), 4.53 (q, $J = 6.9$ Hz, 2H), 3.64 – 3.53 (m, 1H), 1.45 (t, $J = 7.0$ Hz, 3H), 1.00 (s, 3H), 0.56 (s, 3H). ^{13}C NMR (100 MHz, CDCl_3) δ 164.81, 164.14, 153.91, 140.72, 135.32, 132.12, 129.99, 124.35, 121.57, 116.36, 115.59, 91.56, 72.19, 63.25, 58.45, 56.88, 50.21, 45.62, 41.95, 38.18, 37.26, 36.58, 32.18, 31.90, 31.34, 29.71, 25.01, 24.72, 20.86, 19.43, 14.55, 13.15. HRMS (ESI): m/z calcd for $\text{C}_{33}\text{H}_{40}\text{BrN}_2\text{O}_2$ ($\text{M}+\text{H}$) $^+$ 575.2273; found, 575.2271 .

4.2.18. 2-Ethoxyl-3-cyano-4-(4-methylphenyl)-6-[(3 β , 17' β)-3'-(hydroxyl) androst-5'-en-17'-yl]pyridine (**4d**)

White solid, yield 27%, m.p.110.1-111.9 $^{\circ}\text{C}$. ^1H NMR (400 MHz, CDCl_3) δ 7.49 (d, $J = 7.8$ Hz, 2H), 7.29 (d, $J = 8.0$ Hz, 2H), 6.80 (s, 1H), 5.36 (s, 1H), 4.53 (q, $J = 7.0$ Hz, 2H), 3.65 - -3.43 (m, 1H), 2.41 (s, 3H), 1.46 – 1.44 (m, 3H), 1.00 (s, 3H), 0.56 (s, 3H). ^{13}C NMR (100 MHz, CDCl_3) δ 167.21, 164.27, 155.24, 140.74, 139.96, 133.61, 129.58, 128.31, 121.60, 116.59, 116.00, 91.34, 72.21,

63.05, 58.42, 56.88, 50.88, 50.25, 46.34, 45.55, 41.96, 38.19, 37.27, 36.59, 34.89, 32.62, 32.19, 31.33, 29.71, 27.43, 26.46, 24.74, 21.36, 20.88, 19.41, 14.74, 14.58, 13.13. HRMS (ESI):m/z calcd for $C_{34}H_{42}N_2O_2Na$ (M+Na)⁺ 533.3144; found, 533.3145.

4.2.19. 2-Ethoxyl-3-cyano-4-(3-bromophenyl)-6-[(3' β , 17' β)-3'-(hydroxyl) androst-5'-en-17'-yl]pyridine (**4e**)

White solid, yield 29%, m.p.90.7-93.3 \square . ¹H NMR (400 MHz, CDCl₃) δ 7.66 (s, 1H), 7.61 (d, J = 8.0 Hz, 1H), 7.54 (d, J = 7.8 Hz, 1H), 7.37 (t, J = 7.9 Hz, 1H), 6.77 (s, 1H), 5.37 (s, 1H), 4.54 (d, J = 7.1 Hz, 2H), 3.65 – 3.49 (m, 1H), 1.45 (t, J = 8.0 Hz, 3H), 1.00 (s, 3H), 0.56 (s, 3H). ¹³C NMR (100 MHz, CDCl₃) δ 167.78, 164.87, 164.07, 153.52, 140.75, 138.48, 132.70, 131.20, 130.40, 127.16, 122.86, 121.56, 116.46, 115.35, 91.79, 72.11, 63.27, 58.47, 56.89, 50.22, 45.72, 41.99, 38.19, 37.26, 36.59, 32.18, 31.41, 29.70, 29.24, 25.04, 24.72, 20.85, 19.40, 14.53, 13.15. HRMS (ESI):m/z calcd for $C_{33}H_{39}BrN_2O_2Na$ (M+Na)⁺ 597.2093; found, 597.2091.

4.2.20. 2-Ethoxyl-3-cyano-4-(3-nitrophenyl)-6-[(3' β , 17' β)-3'-(hydroxyl) androst-5'-en-17'-yl]pyridine (**4f**)

White solid, yield 30%, m.p.151.9-153.7 \square . ¹H NMR (400 MHz, CDCl₃) δ 8.42 – 8.32 (m, 2H), 7.97 (d, J = 7.7, 1H), 7.72 (t, J = 8.0 Hz, 1H), 6.84 (s, 1H), 5.38 (d, J = 4.9 Hz, 1H), 4.56 (q, J = 7.0 Hz, 1H), 3.73 – 3.64 (m, 1H), 1.47 (t, J = 7.0 Hz, 3H), 1.01 (s, 3H), 0.58 (s, 3H). ¹³C NMR (100 MHz, CDCl₃) δ 165.67, 164.19, 152.61, 148.50, 140.31, 138.00, 134.45, 130.14, 124.45, 123.41, 121.93, 116.40, 115.17, 91.69, 73.33, 63.52, 58.55, 56.89, 50.15, 45.77, 41.61, 38.19, 37.18, 36.54, 32.17, 31.93, 31.87, 31.07, 29.70, 29.36, 25.08, 24.71, 22.69, 20.85, 19.39, 17.88, 14.50, 14.12, 13.19. HRMS (ESI):m/z calcd for $C_{33}H_{39}N_3O_4Na$ (M+Na)⁺ 564.2838; found, 564.2837.

4.2.21. 2-Ethoxyl-3-cyano-4-(3,5-difluorophenyl)-6-[(3' β , 17' β)-3'-(hydroxyl) androst-5'-en-17'-yl]pyridine (**4g**)

White solid, yield 32%, m.p.90.1-91.9 \square . ¹H NMR (400 MHz, CDCl₃) δ 7.10 (d, J = 5.6 Hz, 2H), 6.98 – 6.88 (m, 1H), 6.76 (s, 1H), 5.37 (d, J = 4.4 Hz, 1H), 4.55 (q, J = 7.0 Hz, 2H), 3.59-3.53 (m, 1H), 1.46 (t, J = 7.0 Hz, 3H), 1.01 (s, 3H), 0.56 (s, 3H). ¹³C NMR (100 MHz, CDCl₃) δ 165.18, 164.09, 161.83, 152.63, 140.76, 121.52, 116.26, 114.99, 111.83, 111.57, 105.08, 91.74, 72.45, 72.11, 63.38, 58.50, 56.90, 50.22, 45.68, 42.03, 38.19, 37.26, 36.58, 32.18, 31.92, 31.43, 29.69,

29.36, 25.02, 24.70, 22.68, 20.84, 19.40, 14.48, 14.10, 13.13. HRMS (ESI):m/z calcd for $C_{33}H_{39}F_2N_2O_2$ (M+H)⁺ 533.2980; found, 533.2977.

2.2.22. 2-Ethoxyl-3-cyano-4-(4-methylsulfonylphenyl)-6-[(3' β , 17' β)-3'-(hydroxyl) androst-5'-en-17'-yl]pyridine (**4h**)

White solid, yield 30%, m.p.85.3-87.8 \square . ¹H NMR (400 MHz, CDCl₃) δ 8.08 (d, J = 8.5 Hz, 2H), 7.77 (d, J = 8.5 Hz, 2H), 6.76 (s, 1H), 5.37 (d, J = 5.0 Hz, 1H), 4.54 (q, J = 7.1 Hz, 2H), 3.67 – 3.52 (m, 1H), 3.12 (s, 3H), 1.47 (t, J = 8.0 Hz, 3H), 1.00 (s, 3H), 0.99 (s, 3H). ¹³C NMR (100 MHz, CDCl₃) δ 168.34, 164.24, 152.88, 141.77, 141.56, 140.68, 129.52, 128.02, 121.58, 116.87, 115.22, 91.48, 72.12, 63.45, 57.29, 54.83, 50.98, 49.94, 46.55, 44.53, 42.00, 37.16, 36.56, 34.97, 32.59, 32.27, 31.92, 31.41, 29.69, 29.66, 29.36, 27.49, 26.42, 22.69, 21.00, 20.86, 19.39, 14.66, 14.12. HRMS (ESI):m/z calcd for $C_{34}H_{42}N_2O_4SNa$ (M+Na)⁺ 597.2763; found, 597.2761.

4.2.23. 2-Ethoxyl-3-cyano-4-(4-fluorophenyl)-6-[(3' β , 17' β)-3'-(hydroxyl) androst-5'-en-17'-yl]pyridine (**4i**)

White solid, yield 33%, m.p.106.1-107.7 \square . ¹H NMR (400 MHz, CDCl₃) δ 7.64 – 7.45 (m, 2H), 7.18 (t, J = 8.3 Hz, 1H), 6.99 (s, 1H), 6.84 – 6.71 (s, 1H), 5.34 (d, J = 9.5 Hz, 1H), 4.52 (q, J = 7.5, 2H), 3.57 – 3.43 (m, 1H), 1.44 (t, J = 4.0 Hz, 3H), 1.00 (s, 3H), 0.56 (s, 3H). ¹³C NMR (100 MHz, CDCl₃) δ 164.61, 164.19, 164.09, 160.29, 154.77, 154.03, 141.03, 130.45, 130.37, 129.82, 129.30, 128.51, 121.28, 116.54, 116.39, 116.15, 116.08, 115.86, 115.69, 114.79, 114.48, 91.71, 91.32, 71.49, 63.63, 63.17, 63.00, 58.42, 58.38, 56.88, 50.28, 50.26, 49.96, 45.58, 45.50, 42.22, 38.19, 37.32, 36.60, 36.57, 32.19, 31.90, 31.54, 29.27, 25.00, 24.98, 24.72, 20.96, 20.86, 19.42, 14.78, 14.73, 14.57, 14.54, 13.12, 13.11. HRMS (ESI):m/z calcd for $C_{33}H_{40}FN_2O_2$ (M+H)⁺ 515.3074; found, 515.3076.

2.2.24. 2-Ethoxyl-3-cyano-4-(pyridine-3-yl)-6-[(3' β , 17' β)-3'-(hydroxyl) androst-5'-en-17'-yl]pyridine (**4j**)

White solid, yield 23%, m.p.105.4-107.2 \square . ¹H NMR (400 MHz, CDCl₃) δ 8.78 (s, 1H), 8.77 (s, 1H), 8.01 (s, 1H), 7.46 (s, 1H), 6.78 (s, 1H), 5.37 (d, J = 5.4 Hz, 1H), 4.55 (q, J = 7.2 Hz, 2H), 3.56 – 3.46 (m, 1H), 1.47 (t, J = 8.0 Hz, 3H), 1.01 (s, 3H), 0.57 (s, 3H). ¹³C NMR (100 MHz, CDCl₃) δ 168.09, 165.18, 164.27, 151.54, 151.36, 150.69, 148.87, 140.92, 135.89, 132.49, 123.49, 121.43,

116.76, 116.40, 91.73, 71.69, 63.35, 58.51, 57.27, 56.91, 50.96, 50.23, 49.95, 46.49, 45.69, 42.27, 42.23, 38.20, 37.29, 36.61, 34.98, 32.59, 32.20, 31.89, 31.61, 27.44, 26.92, 26.42, 25.01, 24.74, 20.99, 19.42, 14.50, 13.14. HRMS (ESI):m/z calcd for C₃₂H₃₉N₃O₂Na (M+Na)⁺ 520.2940 ; found, 520.2941.

4.2.25. 2-Ethoxyl-3-cyano-4-(thiofuran-2-yl)-6-[(3' β , 17' β)-3'-(hydroxyl) androst-5'-en-17'-yl]pyridine (**4k**)

White solid, yield 34%, m.p.91.1-93.1 \square .¹H NMR (400 MHz, CDCl₃) δ 7.88 (s, 1H), 7.50 (s, 1H), 7.18 (s, 1H), 6.90 (s, 1H), 5.37 (t, *J* = 5.8 Hz, 1H), 4.56 – 4.47 (m, 2H), 3.60 – 3.46 (m, 1H), 1.45 (t, *J* = 7.0 Hz, 3H), 0.99 (s, 3H), 0.55 (s, 3H). ¹³C NMR (100 MHz, CDCl₃) δ 167.48, 164.43, 146.53, 140.90, 137.90, 129.14, 128.58, 121.49, 115.44, 89.62, 71.72, 63.18, 58.34, 56.90, 50.26, 46.41, 45.61, 42.22, 38.13, 37.29, 36.57, 34.85, 32.61, 32.18, 31.91, 31.63, 27.35, 26.43, 24.91, 24.72, 20.86, 19.44, 14.55, 13.11. HRMS (ESI):m/z calcd for C₃₁H₃₈N₂O₂SNa (M+Na)⁺ 525.2552 ; found, 525.2553.

4.2.26. 2-Ethoxyl-3-cyano-4-(thiofuran-3-yl)-6-[(3' β , 17' β)-3'-(hydroxyl) androst-5'-en-17'-yl]pyridine (**4l**)

White solid, yield 27%, m.p.86.4-88.2 \square .¹H NMR (400 MHz, CDCl₃) δ 8.18 (s, 1H), 7.54 (s, 1H), 6.87 (s, 1H), 6.81 (s, 1H), 5.37 (s, 1H), 4.51 (q, *J* = 7.5 Hz, 2H), 3.58 – 3.48 (m, 1H), 1.44 (t, *J* = 7.0 Hz, 3H), 1.00 (s, 3H), 0.54 (s, 3H). ¹³C NMR (100 MHz, CDCl₃) δ 221.24, 167.51, 164.55, 145.52, 143.88, 142.79, 140.92, 121.98, 121.43, 120.90, 116.43, 114.97, 114.61, 109.33, 88.82, 71.68, 63.04, 58.36, 56.89, 51.77, 50.26, 45.54, 42.20, 38.17, 37.28, 36.60, 35.85, 34.85, 32.17, 31.61, 30.79, 27.42, 26.43, 24.70, 21.89, 20.85, 19.43, 14.54, 13.55, 13.09. HRMS (ESI):m/z calcd for C₃₁H₃₈N₂O₂SNa (M+Na)⁺ 525.2552 ; found, 525.2551.

4.3. General procedure for the synthesis of compound **5j**

A mixture of compound **3j** (1.0mmol), acetic anhydride (1.2mmol), 4-dimethylaminopyridine (DMAP, 0.02mmol) and Et₃N (1.0mmol) in dichloromethane (5 mL) was stirred for about 5h at room temperature. After completion of the reaction as evident from TLC, the organic phase concentrated under reduced vacuum. The residue was purified by column chromatography (PE: Acetone = 4:1) to give compound **5j**, White solid, yield 90%, m.p.92.2-94.0 \square .¹H NMR (400 MHz,

CDCl_3) δ 8.85 (d, $J = 1.6$ Hz, 1H), 8.64 (d, $J = 4.7$ Hz, 1H), 7.96 – 7.82 (m, 1H), 7.38 (d, $J = 7.9$, 1H), 6.82 (s, 1H), 6.71 (s, 1H), 5.41 (d, $J = 4.9$ Hz, 1H), 4.69 – 4.53 (m, 1H), 4.46(q, $J = 7.5$ Hz 2H), 2.03 (s, 3H), 1.41 (t, $J = 4.0$ Hz, 3H), 1.02 (s, 3H), 0.56 (s, 3H). ^{13}C NMR (100 MHz, CDCl_3) δ 170.52, 163.43, 160.35, 149.64, 148.18, 147.39, 139.77, 134.75, 134.38, 123.65, 122.52, 114.21, 105.53, 73.93, 61.58, 58.03, 56.69, 50.26, 44.88, 38.18, 38.12, 37.04, 36.71, 32.16, 31.94, 27.77, 25.05, 24.72, 21.42, 20.82, 19.34, 14.76, 13.03. HRMS (ESI):m/z calcd for $\text{C}_{33}\text{H}_{43}\text{N}_2\text{O}_3$ (M+H)⁺ 515.3274; found, 515.3272.

4.4. Cell proliferation inhibition by MTT assay

About 4×10^3 exponentially growing cells per well were seeded into 96-well plate. After 24 h incubation, the medium was removed and replaced with 200 μL fresh medium containing different concentration of candidate compounds for another 72 h incubation. Then, 20 μL MTT solution (5mg/mL) was added to each well and the cells were then incubated for additional 4 h. Removal of the medium containing MTT, followed by addition of 150 μL DMSO to each well and agitation until the dark blue crystal was dissolved completely. The absorbance was measured using an ELx 800 Universal Microplate Reader (Bio-Tek, Inc.) at a wavelength of 570nm. The date of IC_{50} was analyzed by the software of SPSS 20.

4.5. Colony formation assay

Only about 2000 exponentially growing cells per well were seeded into 6-well plate. After 24 h incubation, the medium was removed and replaced with 3 mL fresh medium containing different concentration of candidate compounds for 7 days incubation. Then, the cell colonies were washed twice by PBS, fixed with 4% paraformaldehyde for 30min, and stained by crystal violet for another 30min. After that, wash away the staining with PBS until the colonies were clear enough.

4.6. Flow cytometric analysis of cell cycle distribution and apoptotic assay

For cell cycle distribution assay, cells were seeded into 6-well plate at 3×10^5 cells per well. After 24h incubation, the cultured medium was replaced with fresh medium containing different concentrations of candidate compound for 48h incubation. Then, the cells were harvested, washed and fixed with 70% ice-cold ethanol at -20°C overnight. Before analyzed by Instrument

LSRForteassa (BD Bioscience, USA), the cells were washed by PBS and stained with RNase and PI (KeyGEN BioTECH, USA) for 30min in dark condition according to the protocol.

For apoptotic assay, after incubation with candidate compound, the cells were harvested and the AnnexinV-FITC/PI apoptosis kit (KeyGEN BioTECH, USA) was used according to the manufacturer's instructions to detect apoptosis cells. About ten thousand events were collected for each sample and analyzed by Instrument LSRForteassa (BD Bioscience, USA).

4.7. Migration and invasion assay

Wound healing assay, transwell assay and matrigel-coated transwell assay were conducted to evaluate the cell migration and invasion ability. For the wound healing assay, exponentially growing cells were seed in 6-well plate at 3×10^5 cells per well. Until the cells density reached 80%~90%, the cell surface was scratched using a 200 μ L pipet tip. Then, the cells were washed and incubated with medium containing different concentration of candidate compound for 48 h, and the cells were photographed on an inverted microscope.

For the transwell assay, exponentially growing cells suspending in 1% FBS and candidate compound contained medium were seed in the upper chamber of Transwell 24-well plate, while fresh 20% FBS and compound contained medium in the lower chamber. After 24 h incubation, remove all the medium, wash the chambers with PBS and the migrating cells were fixed with methanol for 15 min and stained with Hoechst-33258. Each chamber was photographed using Thermo Fisher Cellomics High Content System.

For the matrigel-coated transwell assay, cells were seeded into the Transwell 24-well plate with Matrigel. The medium, attractant, staining and cell counting method were the same as those of the Transwell assay.

4.8. Hoechst 33258 staining

Exponentially growing determined cells were seeded in a 6-well plate at 3×10^5 per well. After 48 h incubation, the medium was replaced with fresh medium containing different concentrations of candidate compound for another 48 h. Then, the cells were washed and fixed with methanol for

about 20 min. Cells were stained with 5 μ g/mL Hoechst-33258 in PBS containing 0.5% Triton X-100 in the dark condition for at least 30min. Apoptosis cells were examined and identified according to the condensation and fragmentation of nuclei by fluorescence microscopy under UV excitation.

4.9. Western blotting analysis

After treated with different concentration of candidate compound for 48 h, the cells were harvested and lysed with cell lysis buffer [1% NP-40, 0.1% sodium dodecyl sulfate (SDS), 150 mM NaCl, 25 mM Tris-HCl, 1% deoxycholic acid sodium salt, 1% PMSF]. Equal amount of cell lysates were denatured, separated by sodium dodecyl sulfate polycrylamide gel electrophoresis (SDS-PAGE), and transferred to 0.22 μ m nitrocellulose membrane. The membrane was blocked with PBS containing 5% nonfat milk for 2 h, and then incubated with the primary antibody overnight at 4 $^{\circ}$ C, followed by incubation with a horseradish peroxidase-conjugated secondary antibody. The immunoblots were visualized by enhanced chemiluminescence kit.

Acknowledgement

This work was supported by National Natural Science Foundation of China (Project No. 81430085, No. 21372206 and No. 81703326); National Key Research Programs of Proteins (No. 2016YFA0501800); Key Research Program of Henan Province (No. 1611003110100); the Starting Grant of Zhengzhou University (No. 32210533).

References

1. D. E. Becker. Basic and Clinical Pharmacology of Glucocorticosteroids. *Anesth. Prog.* 60 (2013) 25-32.
2. D. Kakati, R. K. Sarma, R. Saikia, N. C. Barua, J. C. Sarma. Rapid microwave assisted synthesis and antimicrobial bioevaluation of novel steroidal chalcones. *Steroids* 78 (2013) 321-326.
3. A. E. Amr, M. M. Abdalla, M. M. M. Hussein, H. M. Safwat, M. H. Elgamal. Synthesis and biological activity of some amino-4'-substituted phenyl(pyridine)androst-4-en-3-one candidates. *Russ. J. Gen. Chem.* 87 (2017) 305-310.
4. Z. C. Bin Yu, Shuai Wang, Hong-Min Liu. Recent Advances on the Synthesis and Antitumor Evaluation of Exonuclear Heterosteroids. *Chin. J. Org. Chem.* 37 (2017) 1952-1963.
5. Y. A. Maklad, M. M. Nosseir. Androgenic and anabolic activities of some newly synthesized epiandrosterone and progesterone derivatives. *Sci. Pharm.* 68 (2000) 141-157.
6. Y.-L. Zhang, Y.-F. Li, X.-L. Shi, B. Yu, Y.-K. Shi, H.-M. Liu. Solvent-free synthesis of novel steroidal 2-aminopyridines. *Steroids* 115 (2016) 147-153.
7. Y. Rehman, J. E. Rosenberg. Abiraterone acetate: oral androgen biosynthesis inhibitor for treatment of castration-resistant prostate cancer. *Drug Des. Devel. Ther.* 6 (2012) 13-18.

8. C. J. Ryan , M. R. Smith , J. S. de Bono , A. Molina , C. J. Logothetis , P. de Souza , K. Fizazi , P. Mainwaring , J. M. Piulats , S. Ng , J. Carles , P. F. A. Mulders , E. Basch , E. J. Small , F. Saad , D. Schrijvers , H. Van Poppel , S. D. Mukherjee , H. Suttman , W. R. Gerritsen , T. W. Flaig , D. J. George , E. Y. Yu , E. Efstathiou , A. Pantuck , E. Winquist , C. S. Higano , M.-E. Taplin , Y. Park , T. Kheoh , T. Griffin , H. I. Scher , D. E. Rathkopf. Abiraterone in metastatic prostate cancer without previous chemotherapy. *N. Engl. J. Med.* 368 (2013) 138-148.
9. P. Purushottamachar, A. M. Godbole, L. K. Gediya, M. S. Martin, T. S. Vasaitis, A. K. Kwegyir-Afful, S. Ramalingam, Z. Ates-Alagoz, V. C. O. Njar. Systematic Structure modifications of multitarget prostate cancer drug candidate galeterone to produce novel androgen receptor down-regulating agents as an approach to treatment of advanced prostate cancer. *J. Med. Chem.* 56 (2013) 4880-4898.
10. V. C. Njar, A. M. Brodie. Discovery and development of Galeterone (TOK-001 or VN/124-1) for the treatment of all stages of prostate cancer. *J. Med. Chem.* 58 (2015) 2077-2087.
11. L. Yin, Q. Hu. CYP17 inhibitors [dash] abiraterone, C17,20-lyase inhibitors and multi-targeting agents. *Nat. Rev. Urol.* 11 (2014) 32-42.
12. B. Yu, X.-N. Sun, X.-J. Shi, P.-P. Qi, Y. Fang, E. Zhang, D.-Q. Yu, H.-M. Liu. Stereoselective synthesis of novel antiproliferative steroidal (E, E) dienamides through a cascade aldol/cyclization process. *Steroids* 78 (2013) 1134-1140.
13. B.-L. Zhang, E. Zhang, L.-P. Pang, L.-X. Song, Y.-F. Li, B. Yu, H.-M. Liu. Design and synthesis of novel D-ring fused steroidal heterocycles. *Steroids* 78 (2013) 1200-1208.
14. B. Yu, X.-J. Shi, P.-P. Qi, D.-Q. Yu, H.-M. Liu. Design, synthesis and biological evaluation of novel steroidal spiro-oxindoles as potent antiproliferative agents. *J. Steroid Biochem. Mol. Biol.* 141 (2014) 121-134.
15. Y.-L. Zhang, Y.-F. Li, J.-W. Wang, B. Yu, Y.-K. Shi, H.-M. Liu. Multicomponent assembly of novel antiproliferative steroidal dihydropyridinyl spirooxindoles. *Steroids* 109 (2016) 22-28.
16. Y.-L. Zhang, Y.-F. Li, Y.-K. Shi, B. Yu, G.-C. Zhang, P.-P. Qi, D.-J. Fu, L.-H. Shan, H.-M. Liu. Efficient three-component one-pot synthesis of steroidal polysubstituted anilines. *Steroids* 104 (2015) 1-7.
17. B. Yu, X.-J. Shi, J.-I. Ren, X.-N. Sun, P.-P. Qi, Y. Fang, X.-W. Ye, M.-M. Wang, J.-W. Wang, E. Zhang, D.-Q. Yu, H.-M. Liu. Efficient construction of novel D-ring modified steroidal dienamides and their cytotoxic activities. *Eur. J. Med. Chem.* 66 (2013) 171-179.
18. B. Yu, P.-P. Qi, X.-J. Shi, R. Huang, H. Guo, Y.-C. Zheng, D.-Q. Yu, H.-M. Liu. Efficient synthesis of new antiproliferative steroidal hybrids using the molecular hybridization approach. *Eur. J. Med. Chem.* 117 (2016) 241-255.
19. B. Yu, S.-Q. Wang, P.-P. Qi, D.-X. Yang, K. Tang, H.-M. Liu. Design and synthesis of isatin/triazole conjugates that induce apoptosis and inhibit migration of MGC-803 cells. *Eur. J. Med. Chem.* 124 (2016) 350-360.
20. B. Yu, X.-N. Sun, X.-J. Shi, P.-P. Qi, Y.-C. Zheng, D.-Q. Yu, H.-M. Liu. Efficient synthesis of novel antiproliferative steroidal spirooxindoles via the [3+2] cycloaddition reactions of azomethine ylides. *Steroids* 102 (2015) 92-100.
21. B. Yu, E. Zhang, X.-N. Sun, J.-L. Ren, Y. Fang, B.-L. Zhang, D.-Q. Yu, H.-M. Liu. Facile synthesis of novel D-ring modified steroidal dienamides via rearrangement of 2H-pyrans. *Steroids* 78 (2013) 494-499.
22. B. Yu, D.-Q. Yu, H.-M. Liu. Spirooxindoles: Promising scaffolds for anticancer agents. *Eur. J. Med. Chem.* 97 (2015) 673-698.
23. B. Yu, Y.-C. Zheng, X.-J. Shi, P.-P. Qi, H.-M. Liu. Natural product-derived spirooxindole fragments serve as privileged substructures for discovery of new anticancer agents. *Anti-Cancer Agents Med. Chem.* 16 (2016) 1315-1324.
24. X.-J. Shi, B. Yu, J.-W. Wang, P.-P. Qi, K. Tang, X. Huang, H.-M. Liu. Structurally novel steroidal spirooxindole by 241 potentially inhibits tumor growth mainly through ROS-mediated mechanisms. *Sci. Rep.* 6 (2016) 31607.

25. B. Yu, X.-J. Shi, Y.-F. Zheng, Y. Fang, E. Zhang, D.-Q. Yu, H.-M. Liu. A novel [1,2,4] triazolo [1,5-a] pyrimidine-based phenyl-linked steroid dimer: Synthesis and its cytotoxic activity. *Eur. J. Med. Chem.* 69 (2013) 323-330.
26. Y.-L. Zhang, Y.-F. Li, Y.-K. Shi, B. Yu, G.-C. Zhang, P.-P. Qi, D.-J. Fu, L.-H. Shan, H.-M. Liu. Efficient three-component one-pot synthesis of steroidal polysubstituted anilines. *Steroids*, 104 (2015) 1-7.
27. E. Mann, A. Montero, M. A. Maestro, B. Herradón. Synthesis and crystal structure of peptide-2,2'-biphenyl hybrids. *Helv. Chim. Acta.* 85 (2002) 3624-3638.
28. F. Grein. Twist angles and rotational energy barriers of biphenyl and substituted biphenyls. *J. Phys. Chem. A* 106 (2002) 3823-3827.
29. A. Mazzanti, L. Lunazzi, M. Minzoni, J. E. Anderson. Rotation in biphenyls with a single ortho-substituent. *J. Organic. Chem.* 71 (2006) 5474-5481.
30. K. Bahrami, M. M. Khodaei, F. Naali, B. H. Yousefi. Synthesis of polysubstituted pyridines via reactions of chalcones and malononitrile in alcohols using Amberlite IRA-400 (OH⁻). *Tetrahedron Lett.* 54 (2013) 5293-5298.
31. W.-J. Zhou, S.-J. Ji, Z.-L. Shen. An efficient synthesis of ferrocenyl substituted 3-cyanopyridine derivatives under ultrasound irradiation. *J. Organomet. Chem.* 691 (2006) 1356-1360.
32. J. S. Horoszewicz, S. S. Leong, E. Kawinski, J. P. Karr, H. Rosenthal, T. M. Chu, E. A. Mirand, G. P. Murphy. LNCaP model of human prostatic carcinoma. *Cancer Res.* 43 (1983) 1809-1818.

Highlights

- Compound **3j** exhibited good growth inhibition against PC-3 cells, but was less potent than abiraterone against LNCaP cells
- Compound **3j** inhibited colony formation, migration and evasion of PC-3 cells
- Compound **3j** induced apoptosis of PC-3 cells possibly through the intrinsic apoptotic pathways